HHS Public Access

Author manuscript

Annu Int Conf IEEE Eng Med Biol Soc. Author manuscript; available in PMC 2023 March 28.

Published in final edited form as:

Annu Int Conf IEEE Eng Med Biol Soc. 2022 July ; 2022: 5111–5114. doi:10.1109/EMBC48229.2022.9871052.

High-performance Flexible Microelectrode Array with PEDOT:PSS Coated 3D Micro-cones for Electromyographic Recording

Jiaao Lu[1], **Muneeb Zia**[1] **[Member, IEEE]**, **Matthew J. Williams**[2], **Amanda L. Jacob**[2], **Bryce Chung**[2], **Samuel J. Sober**[2], **Muhannad S. Bakir**[1] **[Senior Member, IEEE]**

[1]Jiaao Lu, Muneeb Zia and Muhannad S. Bakir are with the Department of Electrical and Computer Engineering, Georgia Institute of Technology, Atlanta, GA 30332, USA

[2]Matthew J. Williams, Amanda L. Jacob, Bryce Chung and Samuel J. Sober are with the Department of Biology, Emory University, Atlanta, GA 30322, USA

Abstract

High signal-to-noise ratio (SNR) electromyography (EMG) recordings are essential for identifying and analyzing single-motor unit activity. While high density electrodes allow for greater spatial resolution, the smaller electrode area translates to a higher impedance and lower SNR. In this study, we developed an implantable and flexible 3D microelectrode array with low impedance that enables high-quality EMG recording. We fabricated high-density arrays with large effective surface area, achieved by three-dimentional polyimide micro-cone structure and PEDOT:PSS coating that increases surface roughness. Realized by standard photolithography process, this design can effectively increase effective surface area by up to 250% and significantly improve electrical performance for electrode sites with various geometric surface area, where the electrode impedance is at most improved by 99.3%. EMG activity from mice was recorded by implanting the electrode *in vivo*, and a high SNR with an average of 447.3 was obtained.

I. Introduction

Comparing with central nervous system recording, electromyographic recordings (EMGs) provide more precise and subtle information about muscle movements, that could be critical for specific motor functions characterization and behavioral disease progression [1]. Traditionally, EMGs are collected by inserting fine wire directly into the muscles [2]. However, fine-wire electrodes predominantly capture bulk EMG consisting of activity of multiple units, whereas single motor units are essential for holistic computational analyses [3]. To acquire single-motor unit EMG, two key enablers are high spatial resolution and low electrode impedance. However, these metrics are inherently antagonistic: high spatial resolution demands smaller, densely packed electrode site whereas electrode impedance is negatively impacted by reduced electrode surface area [4].

mbakir@ece.gatech.edu .

One way to address this challenge is to increase the effective surface area (ESA) while maintaining the geometric surface area (footprint). Previous techniques attempting to achieve high ESA for better electrochemical performance can be roughly categorized in two ways: surface modification and 3D structure fabrication. As for surface modification, coating electrode sites with porous conductive polymer by electropolymerization [5] or spincasting [6] is a convenient and effective way to increase surface roughness and thus ESA. Plasma treatment applied on metal surface is an alternative way to modify surface morphology [7]. Fabricating 3D electrodes is another way to increase ESA, yet previous methods either cannot give high density or they utilize fabrication processes that are challenging to be adapted on flexible substrate. The pillars fabricated by Beach et al. [8] with molding technique or the 3D electrode site shaped by reflow of photoresist [3], [9] are all relatively large in dimension. Alternatively, Nick et al. [10] bonded nanoporous membrane to electroplate gold nanopillars and Robinson et al. [11] utilized E-beam lithography and thermal oxide thinning to form vertical pillars, which are both designed for *in vitro* testing on rigid substrate. Combining surface modification and scalable 3D structure fabrication, this paper aims to achieve high-density microelectrode array (MEA) that is flexible and bio-compatible for *in vivo* application.

In this work, the 3D electrode sites are fabricated using polyimide micro-cones that are subsequently coated with PEDOT:PSS to achieve low impedance. We demonstrate the improvement of electrical performance by comparing the impedance between 2D and 3D electrodes with different finishing materials, and show that with the proposed design, the impedance is improved by 99.3% when compared to the planar gold electrode. *In vivo* data of the recorded EMG from mice's digastric muscle is also presented; from the measured EMG a high SNR of 447.3 was calculated, which shows 290% improvement comparing with the previously reported SNR (≈15) for *in vivo* testing [3].

II. Fabrication of 3D MEAs

A. Methods and materials

The fabrication process of 3D microelectrode arrays (MEAs) is summarized in Fig. 1. At first, a 15-μm thick polyimide (PI-2611) layer was spun and cured on a 4-in silicon carrier wafer (Fig. 1(a)). To build 3D polyimide micro-cones, a 15-μm layer of photodefinable polyimide (HD-8820) was spun, soft baked and patterned by a standard photolithography process in a maskless aligner (Fig. 1(b)). The patterned 3D micro-cones were subsequently cured in oven. A reactive ion etch (RIE) process using O_2 and SF_6 (5:1 ratio) plasma was performed to roughen the surface of polyimide substrate and cones. This further increases the surface area and improves the metal adhesion on polyimide. The traces and electrodes were patterned using a lift-off process; a titanium (Ti) adhesion layer followed by gold (Au) were deposited using evaporation process. A thin sacrificial Ti layer was also deposited on the gold as a means to visually identify successful etch of the top polyimide layer. (Fig. 1(c)). A 5-μm polyimide (PI-2611) was then spin coated and cured in oven. An etch mask was patterned using a 6-μm thick positive photoresist (PR) and the top polyimide was then etched using RIE to expose the electrode and connector sites (Fig. 1(d)). The MEAs were

subsequently diced using a femtosecond laser (Fig. 1(e)). A 32-channel Omnetics connector was then connected to each array using anisotropic conductive film (ACF) (Fig. 1(f)).

To further improve the electrical performance, a PEDOT:PSS layer was deposited onto the gold microelectrodes via electropolymerization [5]. An aqueous dispersion of 10mM EDOT added to 2.0g/100mL NaPSS was used as electrolyte to electropolymerize PEDOT:PSS under galvanostatic conditions in a two-electrode setup, where the gold electrode array served as working electrode and a platinum mesh as counter/reference electrode. A constant current of current density 0.5 mA/cm^2 was applied for 5 min to deposit a layer of PEDOT:PSS under room temperature.

B. Fabrication results

The PEDOT:PSS coated 3D polyimide micro-cones were successfully fabricated in electrodes with various footprint sizes (from 200μm×200μm to 5μm×5μm). An optical image of fabricated MEA is shown in Fig. 2(a). The surface morphology of PEDOT:PSS covered cones was examined with a field emission scanning electron microscope (SEM), and an example of 20μm×20μm electrode is shown in Fig. 2(b). The conical shape of the 3D micro-structure is achieved by tuning the exposure and development process for the photodefinable polyimide. The addition of 3D micro-cones results in an increase in ESA by 150% to 250% for different footprint sizes. Electrodeposited PEDOT:PSS uniformly covered the 3D micro-cones, forming a rough and porous coating to further enhance the ESA. The cross-sectional view in Fig. 2(c) clearly reveals the different layers of the electrode: the substrate and cone made of polyimide, thin trace metal, and the top PEDOT of the thickness in the order of 1 μm.

III. Characterization and EMG measurement

A. Electrochemical characterization

In order to evaluate the benefits of added 3D structure and porous PEDOT:PSS coating, impedance at 1kHz of planar and 3D electrodes both with gold and PEDOT:PSS finishing layers were obtained in a 2-electrode setup in physiological saline solution (0.9% NaCl) using a Ag/AgCl reference electrode. We compared the average impedance (n=8) of electrode sites across eight different sizes from 200μm×200μm to 5μm×5μm as shown in Fig. 3. Electrodes with 3D micro-cones show a significant impedance reduction in all footprint sizes for both gold and PEDOT:PSS surface finishes. The PEDOT:PSS coating further reduces the impedance of the 3D micro-cone electrodes when compared to the gold electrodes, which aligns with previous observation [5]. For 10μm×10μm electrode sites, the PEDOT:PSS coated 3D micro-cone electrode show a 99.3% reduction in impedance as compared to planar gold electrodes. The smallest fabricated 3D micro-cone electrode with PEDOT:PSS coating, with a size of 5μm×5μm, has an average impedance of 146.5 kOhm; this is equivalent to the impedance of a 80μm×80μm 2D gold electrode.

We further validated the decrease of impedance through comparing the electrochemical impedance spectroscopy (EIS) results between planar gold and 3D PEDOT:PSS coated micro-cone electrodes with representative footprint sizes, as shown in Fig. 4. The

experiments were conducted in saline solution with a 3-electrode system with Ag/AgCl reference and platinum mesh counter electrodes. The changes in impedance magnitude is consistent with our results at 1 kHz, as the 3D micro-cones together with PEDOT coating significantly reduce the impedance value over the tested frequency range from 0.1 Hz to 100 kHz for all sizes.

Cyclic voltammetry measurements were also carried out with the same 3-electrode setup to determine the charge storage capacity (CSC) of the fabricated 3D micro-cone electrodes. The CV results of 3D micro-cone electrode with footprint of 200μm×200μm is shown in Fig. 5 and the CSC is calculated to be 34.2 mC/cm^{-2}. This demonstrates its feasibility for stimulation application with the measured CSC comparable or better than some of the published stimulation electrodes [12], [13].

B. EMG measurement and data analysis

The fabricated 3D MEAs with micro-cones were utilized to record EMG activity from digastric muscles of anesthetized mice. All procedures were approved by the Emory University Institutional Animal Care and Use Committee. After the adult C57BL/6J male mice (2) were anesthetized (4% (vol/vol) isoflurane in oxygen gas) to a proper depth, an incision was made under the jaw, and skin was removed to reveal the digastric muscle. The electrode array was placed on the muscle's surface to collect spontaneously-occurring motor unit activity through the Omnetics connector, which interfaces with a 32 channel RHD recoding headstage containing a digital amplifier (RHD2132; Intan Technologies). EMG signals were recorded on a computer at 30 Hz through a RHD USB Interface Board (Part C3100; Intan Technologies).

Waveforms from different motor units were identified using standard methods that use principal component analysis (PCA) and k-means to cluster waveforms with similar shapes [14]. The amplitude of each spike cluster was measured by the average peak of each waveform in that cluster. The noise level of each channel was measured by the root mean square (RMS) of a one-minute section of signal not containing any spikes. The SNR for each spike was then computed by dividing the amplitude of each spike cluster by the noise level on the corresponding channel.

$$SNR = \left| \frac{V_{peak}}{noise_{RMS}} \right| \quad (1)$$

High-quality EMG recordings were successfully obtained from mice with the low-impedance 3D MEAs, in which both single and multiple motor units were detected (Fig. 6). In single motor unit recording, the device were able to detect small differences in the action potential's timing and amplitude, which indicate that the electrode has high temporal and spatial resolution to distinguish the different locations of electrode contacts relative to the active muscle fibers. These variations across channels allow multiple motor units to be isolated from single recordings. The multiple motor units recording further showed that our device has significantly higher SNR when comparing with other papers [3]. We achieved a

mean SNR value of **203.3** for the motor unit with the smaller spike, as well as a mean SNR of **447.3** for the motor unit with the larger spike (Fig. 6(b) top).

IV. Conclusion

In this paper, we present a flexible and bio-compatible microelectrode array with 3D micro-cones and PEDOT:PSS coating that gives high SNR in *in vivo* experiments. Through the proposed novel fabrication process, we built micro-cones with photodefinable polyimide that increases the effective surface area up to 250% larger. Electrochemical characterization was performed for electrode with various sizes, where the impedance of our device consistently outperform benchmark devices in tested frequency range. Specifically, the impedance at 1kHz is reduced by two orders of magnitude. The cyclic voltammetry results show a CSC value of 34.2 mC/cm^2 for 200μm×200μm electrode, which shows potential for stimulation applications. The 3D micro-cone electrodes were successfully implanted in mice digastric muscles to obtain acute data, where a SNR of 447.3 was measured through multiple motor units recording. With the high SNR achieved, our device provides a promising approach for the successful acquisition and analysis of single motor unit activity.

Acknowledgment:

This work was funded by NIH grants R01NS084844, R01NS099375, R01NS109237, and the McKnight Foundation and was performed in part at the GA Tech Institute for Electronics and Nanotechnology.

References

[1]. Tysseling VM, Janes L, Imhoff R, Quinlan KA, Lookabaugh B, Ramalingam S, Heckman C, and Tresch MC, “Design and evaluation of a chronic emg multichannel detection system for long-term recordings of hindlimb muscles in behaving mice,” J. Electromyogr. Kinesiol, vol. 23, no. 3, pp. 531–539, 2013. [PubMed: 23369875]

[2]. Warren GL, Ingalls CR, Shah SJ, and Armstrong R, “Uncoupling of in vivo torque production from emg in mouse muscles injured by eccentric contractions,” J. Physiol, vol. 515, no. 2, pp. 609–619, 1999. [PubMed: 10050026]

[3]. Zia M, Chung B, Sober S, and Bakir MS, “Flexible multielectrode arrays with 2-d and 3-d contacts for *in˜vivo* electromyography recording,” IEEE Trans. Compon. Packag. Manuf. Technol, vol. 10, no. 2, pp. 197–202, 2020.

[4]. Seker E, Berdichevsky Y, Begley MR, Reed ML, Staley KJ, and Yarmush ML, “The fabrication of low-impedance nanoporous gold multiple-electrode arrays for neural electrophysiology studies,” Nanotechnology, vol. 21, no. 12, p. 125504, 2010. [PubMed: 20203356]

[5]. Gerwig R, Fuchsberger K, Schroeppel B, Link GS, Heusel G, Kraushaar U, Schuhmann W, Stett A, and Stelzle M, “Pedot–cnt composite microelectrodes for recording and electrostimulation applications: fabrication, morphology, and electrical properties,” Front. Neuroeng, vol. 5, p. 8, 2012. [PubMed: 22586394]

[6]. Koutsouras DA, Hama A, Pas J, Gkoupidenis P, Hivert B, Faivre-Sarrailh C, Di Pasquale E, Owens RM, and Malliaras GG, “Pedot: Pss microelectrode arrays for hippocampal cell culture electrophysiological recordings,” MRS Commun., vol. 7, no. 2, pp. 259–265, 2017.

[7]. Chung T, Wang J, Wang J, Cao B, Li Y, and Pang S, “Electrode modifications to lower electrode impedance and improve neural signal recording sensitivity,” J. Neural Eng, vol. 12, no. 5, p. 056018, 2015. [PubMed: 26394650]

[8]. Beach S, Grundeen S, Doyle A, and Theogarajan L, “Fabrication and validation of flexible 3d pillar electrodes for neural electrophysiological recording,” ERX, vol. 2, no. 2, p. 025025, 2020.

[9]. Rui Y, Liu J, Wang Y, and Yang C, “Parylene-based implantable pt-black coated flexible 3-d hemispherical microelectrode arrays for improved neural interfaces,” Microsyst. Technol, vol. 17, no. 3, pp. 437–442, 2011.

[10]. Nick C, Quednau S, Sarwar R, Schlaak H, and Thielemann C, “High aspect ratio gold nanopillars on microelectrodes for neural interfaces,” Microsyst. Technol, vol. 20, no. 10-11, pp. 1849–1857, 2014.

[11]. Robinson JT, Jorgolli M, Shalek AK, Yoon M-H, Gertner RS, and Park H, “Vertical nanowire electrode arrays as a scalable platform for intracellular interfacing to neuronal circuits,” Nat. Nanotechnol, vol. 7, no. 3, pp. 180–184, 2012. [PubMed: 22231664]

[12]. Shin S, Kim J, Jeong J, Gwon TM, Choi GJ, Lee SE, Kim J. Jun SB, Chang JW, and Kim SJ, “High charge storage capacity electrodeposited iridium oxide film on liquid crystal polymer-based neural electrodes,” Sens. Mater, vol. 28, no. 3, pp. 243–260, 2016.

[13]. Yang W, Gong Y, Yao C-Y, Shrestha M, Jia Y, Qiu Z, Fan QH, Weber A, and Li W, “A fully transparent, flexible pedot: Pss–ito–ag–ito based microelectrode array for ecog recording,” Lab Chip, vol. 21, no. 6, pp. 1096–1108, 2021 [PubMed: 33522526]

[14]. Sober SJ, Wohlgemuth MJ, and Brainard MS, “Central contributions to acoustic variation in birdsong,” Journal of Neuroscience, vol. 28, no. 41, pp. 10370–10379, 2008. [PubMed: 18842896]

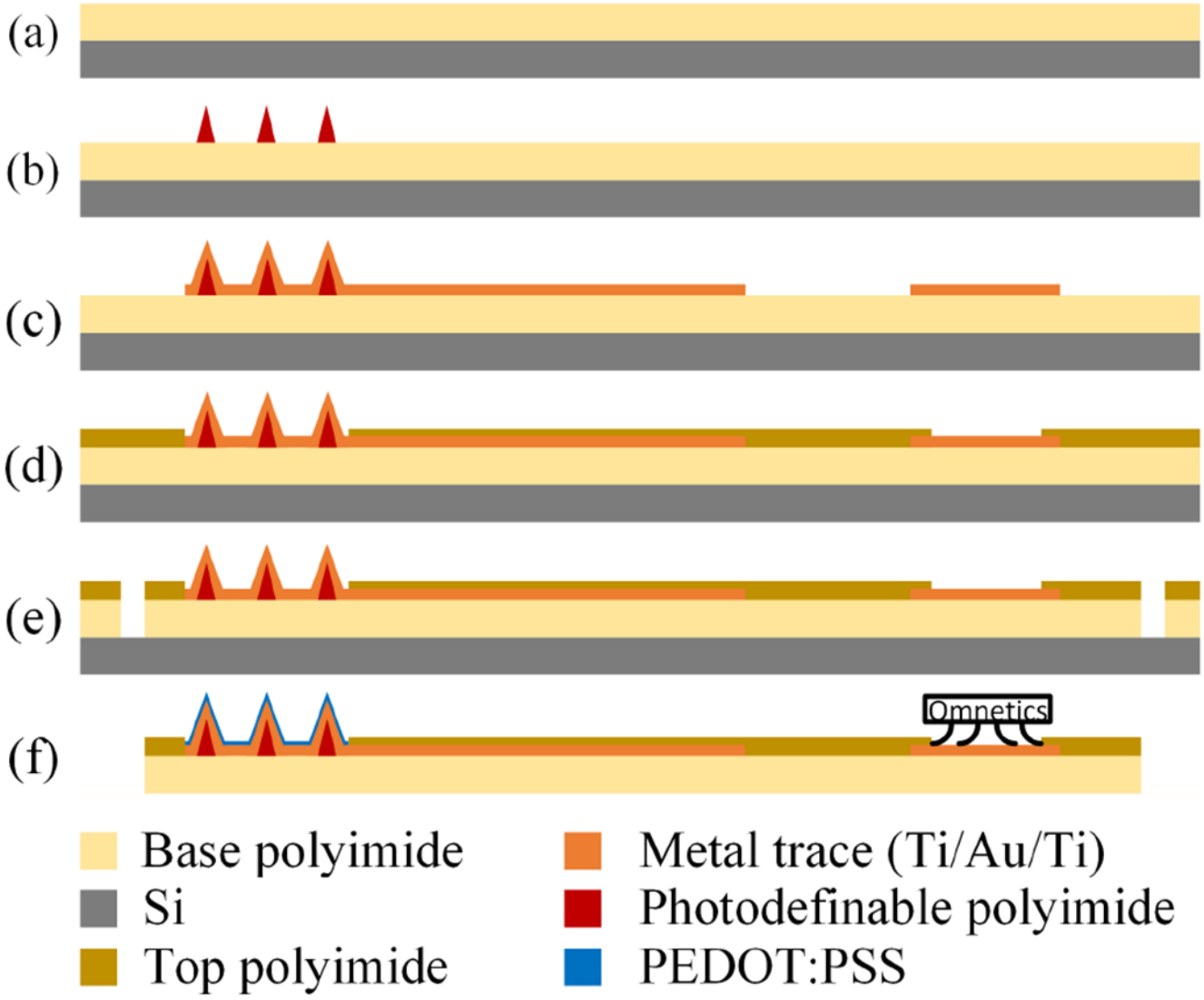

Fig. 1.

Fabrication process of the flexible 3D microelectrode arrays. (a) base polyimide coating, (b) photodefinable polyimide coating and patterning, (c) Ti/Au/Ti evaporation and patterning, (d) top polyimide coating and etching, (e) laser dicing, (f) device release, assembly and electropolymerization of PEDOT.

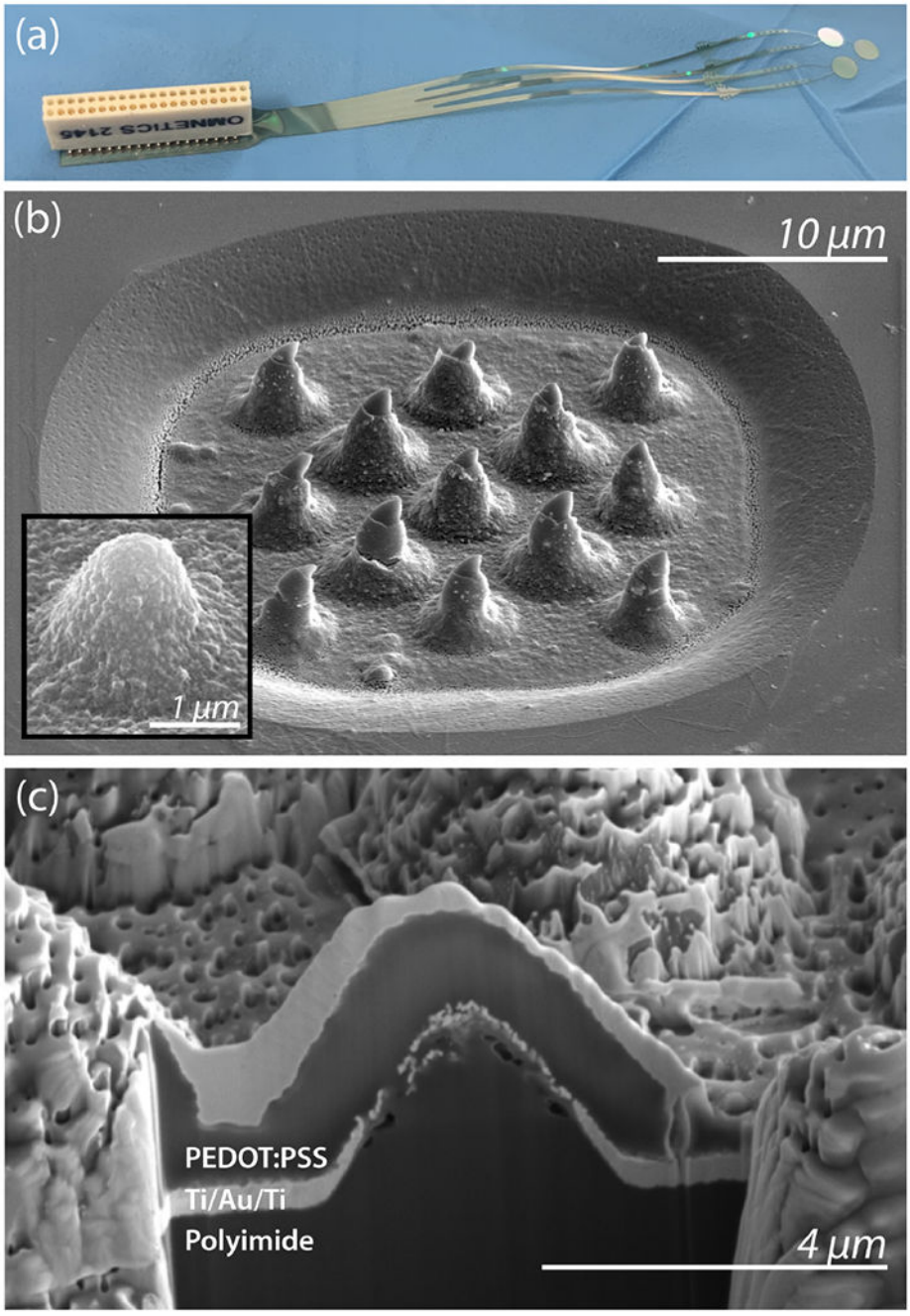

Fig. 2.

Optical and electron microscopy. (a) An optical image of the fabricated 3D MEA. (b) A SEM image of a 20μm×20μm electrode pad with 13 cones on top to increase the effective surface area. The inset picture shows the surface contains nano features and porosity after PEDOT:PSS electropolymerization. (c) The SEM of focused ion beam (FIB) cross-section of the electrode site showing multiple layers of the device. A thin layer of tungsten was deposited on top to protect the surface during FIB.

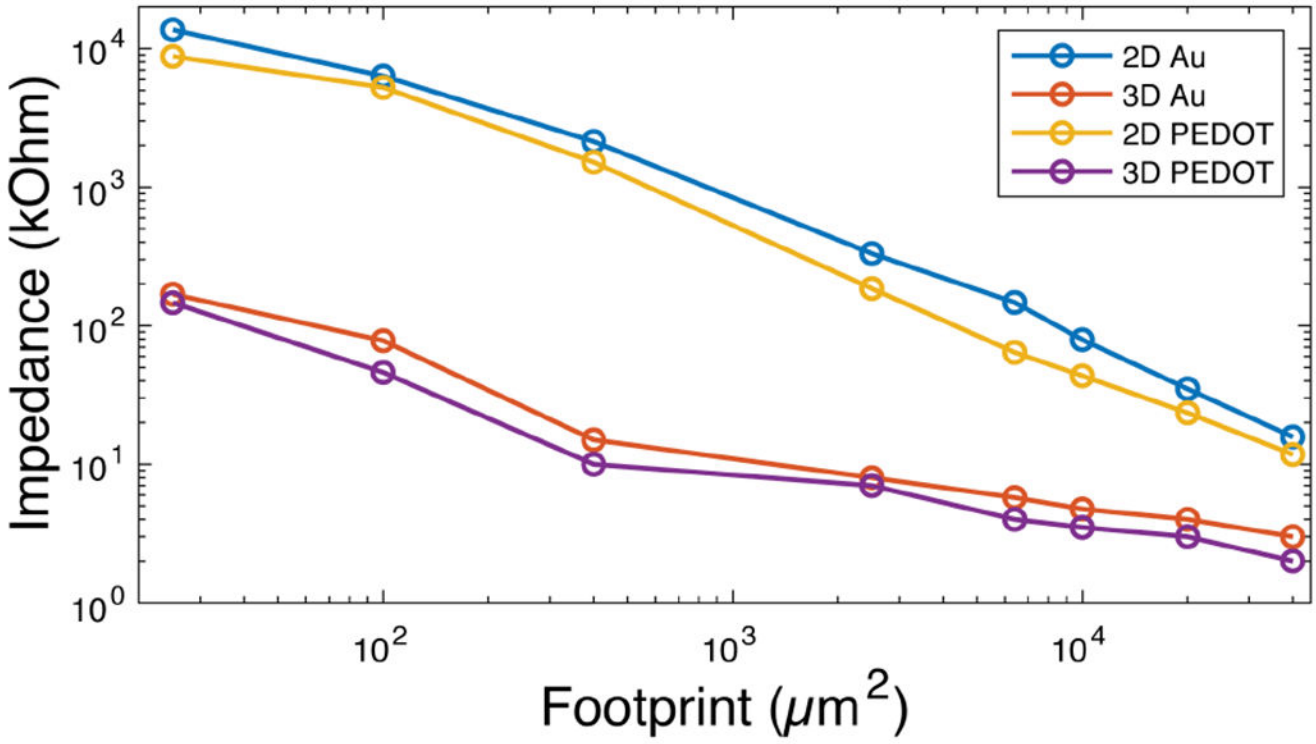

Fig. 3.

Average impedance at 1kHz of eight different footprint areas to show the improvement of 3D structure and porous PEDOT:PSS coating (n=8).

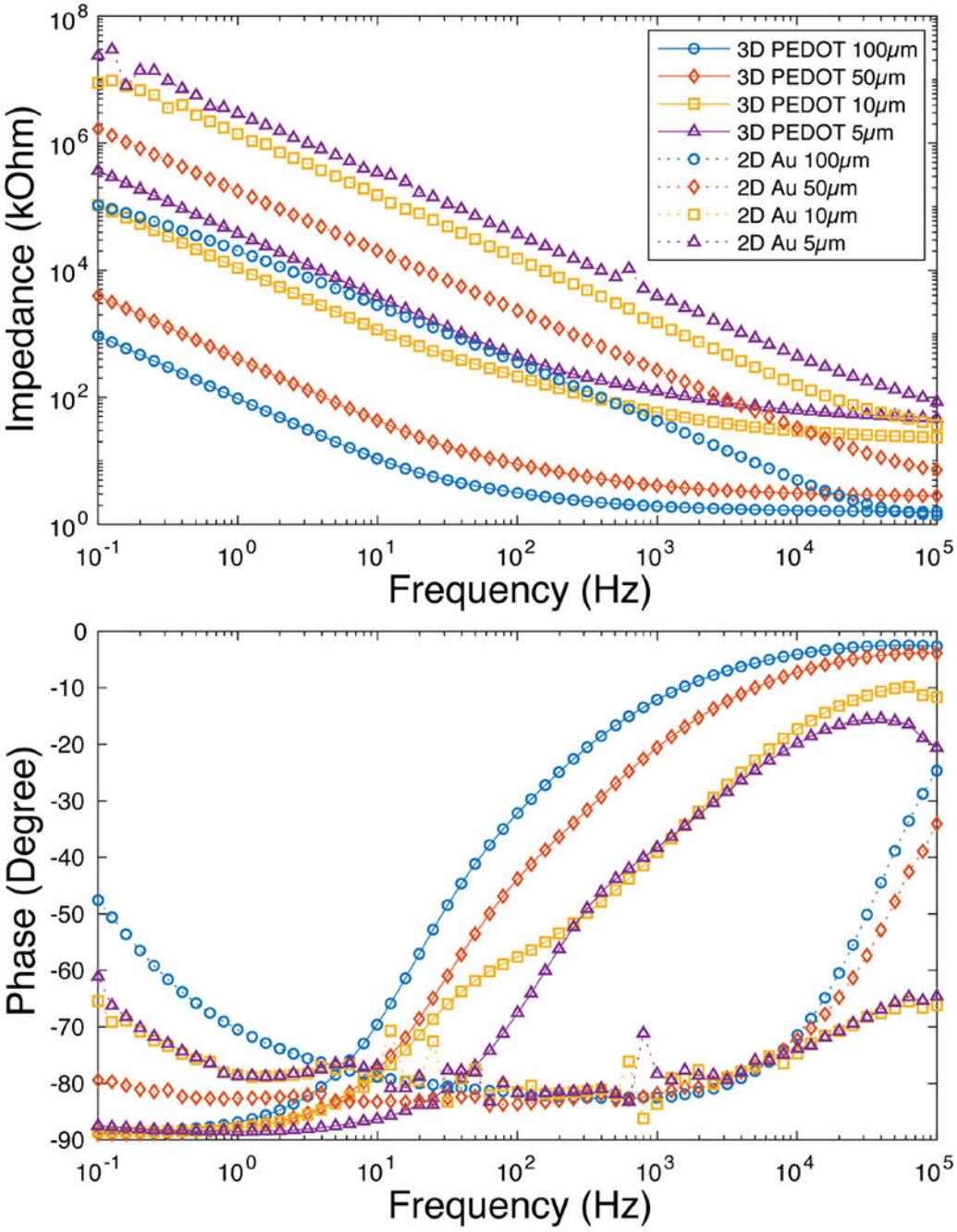

Fig. 4.

EIS measurement of 3D PEDOT:PSS coated microelectrodes and 2D gold microelectrodes with four different footprint sizes.

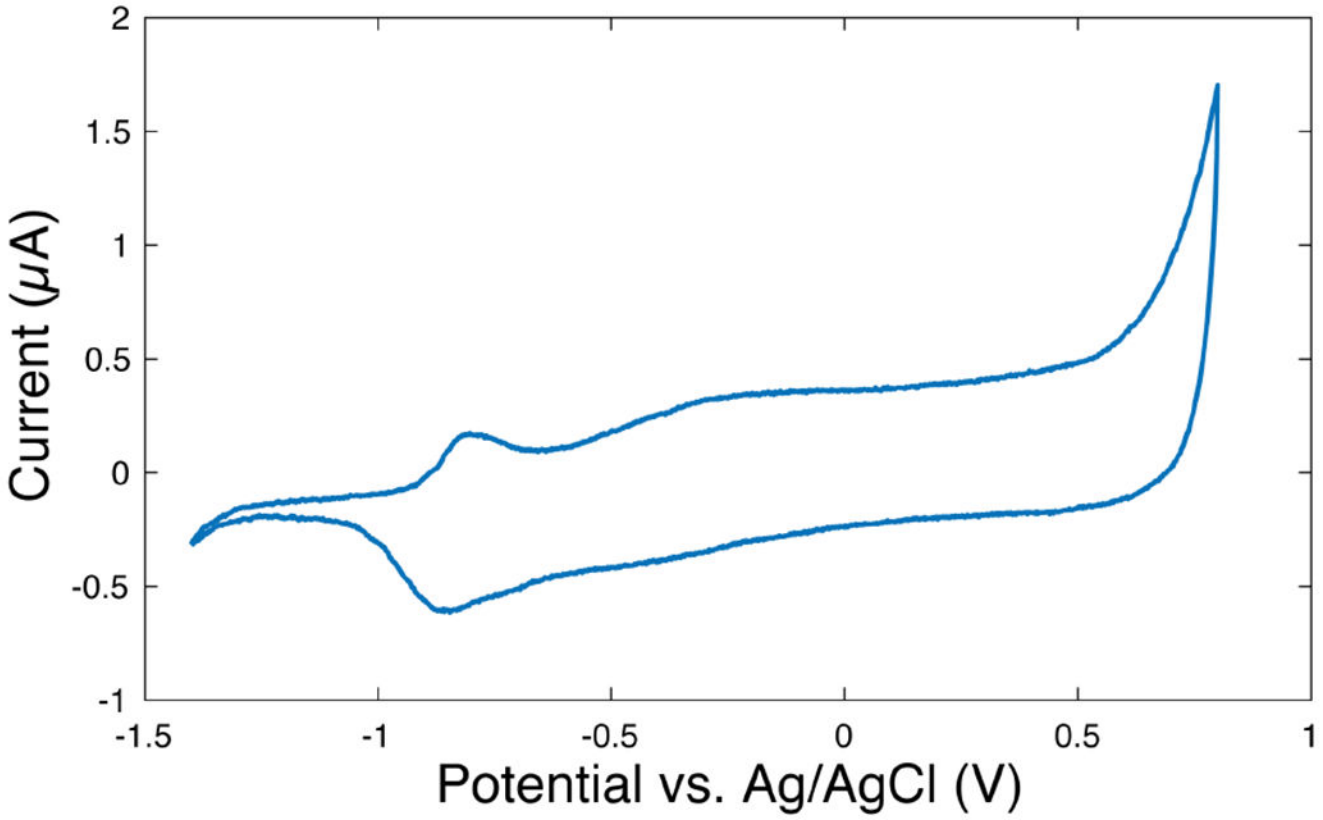

Fig. 5.
Cyclic Voltammetry of PEDOT:PSS coated 3D electrode with side length of 200 μm in saline solution, swept at 100 mV/s.

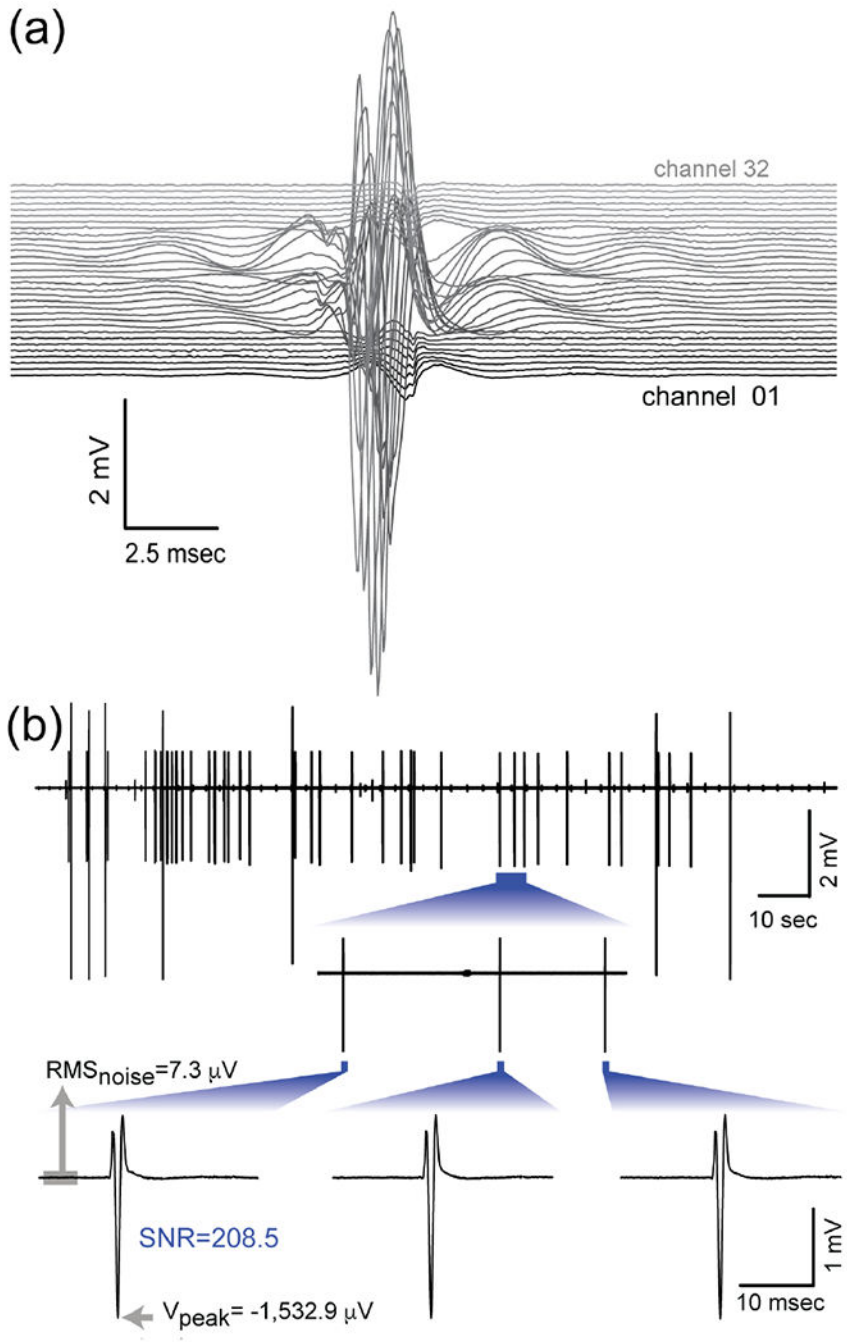

Fig. 6.

High-resolution EMG recordings with micro-cone MEAs. (a) Example recording of a single motor unit from a mouse digastric muscle. Here, a single action potential is detected by roughly half of the electrode array's 32 channels. (b) Recording of multiple motor units from a single MEA channel. Top, recording from the digastric muscle during an epoch in which two different motor units, which can be distinguished visually by their different

amplitudes, were recorded simultaneously. Bottom, detail of three individual spikes and their corresponding SNR values.